Am J Transl Res 2016;8(2):556-567
www.ajtr.org /ISSN:1943-8141/AJTR0018898

Original Article

A time-dependent degeneration manner of condyle in rat CFA-induced inflamed TMJ

Liqin Xu, Huilin Guo, Cheng Li, Jie Xu, Wei Fang, Xing Long

Department of Oral and Maxillofacial Surgery, The State Key Laboratory Breeding Base of Basic Science of Stomatology & Key Laboratory of Oral Biomedicine Ministry of Education, School & Hospital of Stomatology, Wuhan University, Wuhan, Hubei, China

Received October 31, 2015; Accepted December 24, 2015; Epub February 15, 2016; Published February 29, 2016

Abstract: Temporomandibular joint (TMJ) inflammation is a potential risk factor of osteoarthritis (OA) but the detailed degenerative changes in the inflamed TMJ remain unclear. In this study, we evaluated the changes of condylar cartilage and subchondral bone in rat inflamed TMJ induced by Freund's complete adjuvant (CFA). Articular cavity was injected with CFA and the TMJ samples were collected 1, 2, 3, and 4-week post-injection. Hematoxylin & Eosin (H&E) staining, toluidine blue (TB) staining, Safranin O (S.O) staining, Masson trichrome staining and micro-CT were used to assess TMJ degeneration during inflammation. Osteoclast and osteoblast activities were analyzed by tartrate-resistant acid phosphatase (TRAP) staining and osteocalcin (OCN) immunohistochemistry staining respectively. The expression of receptor activator of NF-kB ligand (RANKL) and osteoprotegerin (OPG) in condylar cartilage and subchondral bone was also evaluated through immunohistochemistry and RANKL/OPG ratio was evaluated. Reduced cartilage thickness, decreased number of chondrocytes, and down-regulated proteoglycan expression were observed in the condylar cartilage in the inflamed TMJ. Enhanced osteoclast activity, and expanded bone marrow cavity were reached the peak in the 2-week after CFA-injection. Meanwhile the RANKL/OPG ratio in the cartilage and subchondral bone also increased in the 2-week CFA-injection. Immature, unmineralized new bones with irregular trabecular bone structure, atypical condylar shape, up-regulated OCN expression, and decreased bone mineral density (BMD) were found in the inflamed TMJ. The time-dependent degeneration manner of TMJ cartilage and subchondral bone was found in CFA-induced arthritis rat model. The degeneration in the TMJ with inflammation might be a risk factor and should be concerned.

Keywords: Temporomandibular disorders, cartilage degeneration, subchondral bone remodeling, inflammation, Freund's complete adjuvant

Introduction

Temporomandibular joint osteoarthritis (TMJOA) is a chronic and multi-factorial disorder characterized as synovitis, progressive cartilage degradation, subchondral bone remodeling and chronic pain [1, 2]. Inflammation is believed to be an important risk factor in joint OA, because the concomitant pro-inflammatory factors, including IL-1β, TNF-α, and RANKL, et al., were up-regulated in inflammation and would lead to degenerative changes [3-6]. Futhermore the pro-inflammatory factors were up-regulated in TMJ OA either [7-10]. But as far as TMJOA is concerned, only in a few cases of synovitis will progress into OA eventually and correlative studies merely focused on phenotypic changes in mandibular condyle [11, 12].

It is difficult to perform *in vivo* study of inflamed TMJ in human while Freund's complete adjuvant (CFA) injection is a repeatable and easy method to study the TMJ inflammation. Hence intra-articular TMJ CFA injection is predominantly used to induce joint inflammation [13] and among these CFA-induced TMJ inflammation studies, the detailed degenerative changes of TMJ condyle were not fully evaluated [11, 12]. Hence the detailed degenerative changes of condylar cartilage and subchondral bone during TMJ inflammation should be fully

understood and thereafter the relation between inflamed TMJ and TMJOA might be clear.

Although synovial cells had limited capacity to directly damage bone, they could indirectly induce bone resorption mainly through expressing RANKL viewed as an important cytokines for differentiation and activation of osteoclasts. In addition, previous study showed that synovitis was able to impact the homeostasis of cartilage and subchondral bone [14]. The RANKL and OPG are crucial in the onset and progression of OA [15]. RANKL expressed in the osteoblasts leads to subchondral bone resorption, while OPG expressed in the osteoblasts prevents osteoclastogenesis and accelerates mature osteoclast apoptosis [3]. Hence, RANKL/OPG ratio is widely used to evaluate the degenerative changes of the joint. As to TMJOA, several studies have shown that RANKL and OPG are produced by chondrocytes and different RANKL/OPG ratios can adjust cartilage degradation and subchondral bone remodeling in OA [16, 17]. Cartilage and subchondral bone are protected under decreased RANKL/OPG ratio but adversely affected under increased RANKL/OPG ratio [18, 19].

In the present study, we used CFA-induced inflamed TMJ rat model to examine degenerative changes of TMJ during inflammation and discussed the relationship between inflamed TMJ and TMJOA.

Materials and methods

In this study, all animal experimental procedures were approved by the Ethics Committee for Animal Research, School and Hospital of Stomatology, Wuhan University, China.

Animal experiments

Sixty-four male Sprague-Dawley rats (eight-week-old) obtained from the Experimental Animal Centre of Hubei Province were used. The animals were randomly divided into control and experimental groups. In the experimental group, 50 μL CFA (Sigma-Aldrich, St. Louis, USA.) were injected bilaterally into the anterosuperior compartment of the TMJ according to Kameoka's method [20]. After anesthetized, the zygomatic arch and the base of the zygomatic arch of the rat were palpated and the anterosuperior portion of the zygomatic arch root was identified as the insertion point. The needle was percutaneously inserted into the anterosuperior compartment of the TMJ (**Figure 1Ab**) and the reagent was injected slowly over a time span of 2 min. The control group was received bilateral injections with 50 μL saline.

In the 1, 2, 3 and 4-week post-injection, the rats from two groups were sacrificed respectively (n = 8). At each time point, eight TMJs were selected for micro-computed tomography (Micro-CT) scan and the rest eight TMJs were used for histopathology and immunohistochemistry analyses. The TMJ condyles were collected and fixed in the tubes for Micro-CT scan. For histological staining, the bilateral TMJ tissues including the mandibular condyle, disc, retrodiscal area, and fossa were integrallty dissected and fixed in 4% paraformaldehyde for 24 hours. Following fixation, the tissues were demineralized in 10% ethylene diamine tetraacetic acid (EDTA) for 6 weeks. After decalcification, the TMJ samples were gradient-dehydrated and embedded in paraffin. Continuous mid-sagittal sections of 4 μm were cut parallel to the lateral surface of the condyle and mounted on polylysine-coated slides.

Histological analysis

The TMJ samples were stained with H&E, TB, S.O, Masson trichrome and TRAP in compliance with the manufacturer's protocol. H&E staining was performed to detect the condylar cartilage thickness and chondrocytes number. TB and S.O staining were used to determine proteoglycan changes in the cartilage matrix. Condyle cartilage thickness and proteoglycan area were measured as reported previously [16]. In each section, thickness and proteoglycan area were counted at three regions, that is, the anterior, middle and posterior of condylar cartilage, respectively, and then averaged. Masson trichrome staining was used to observe the trabecula bone morphology change and the degree of bone mineralization [21]. TRAP staining was performed to estimate the osteoclasts activities.

Immunohistochemistry

Immunohistochemical staining for OCN, OPG and RANKL were performed. After de-paraffinized, rehydrated and washed, the sections were then antigen-retrieved by pepsin and incubated with 0.3% hydrogen peroxide for 20 minutes to block endogenous peroxidase activity, followed by processing with serum for 30 minutes to block unspecific ligations. The sections were then treated with rabbit anti-OCN (1:100;

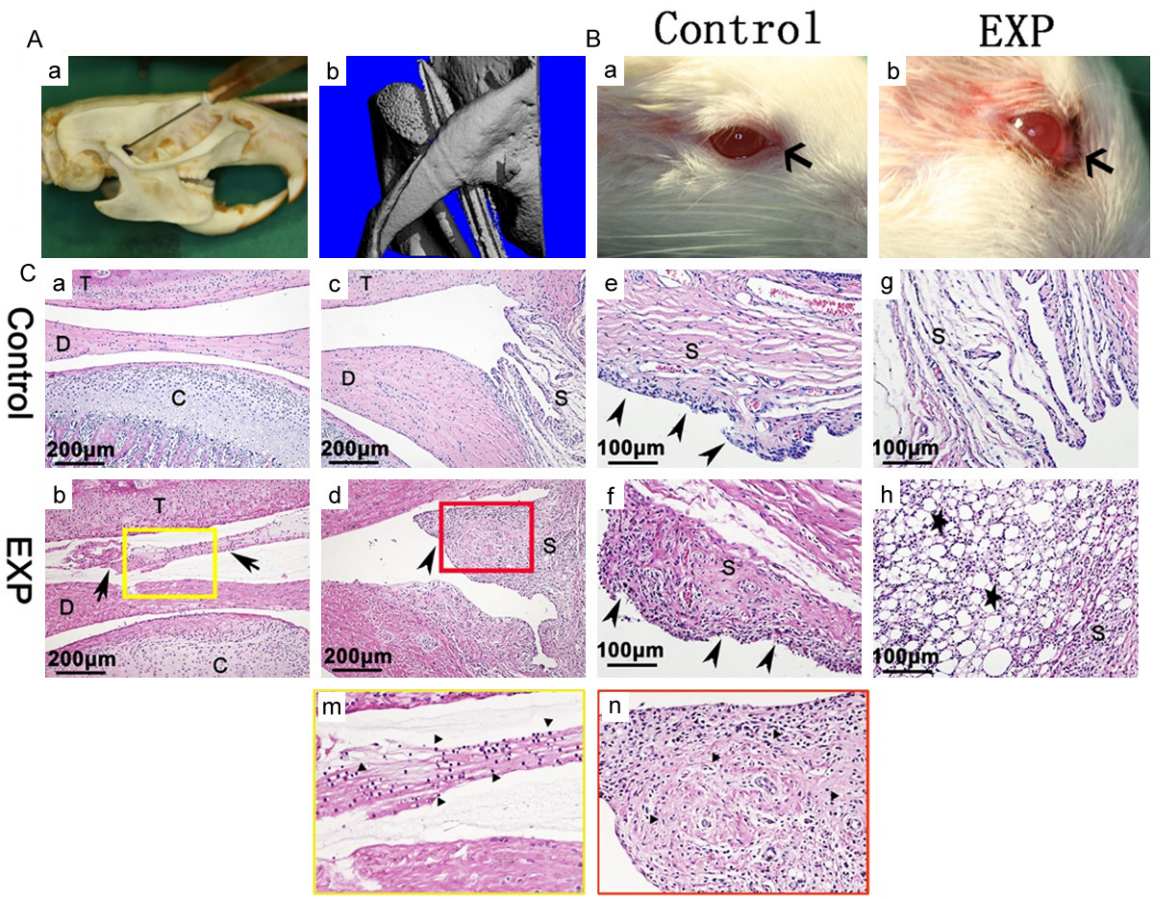

Figure 1. Anterior superior puncture technique and inflammation of TMJ. (A) Anterior superior puncture technique (a), 3D image show the needle tip in the TMJ cavity and just between the base of the zygoma and condylar process (b). (B) Compared with the control group (a), obvious chromodacryorrhea around the eyelid (b) (arrow) was appeared in experiment group. (C) In contrast with control group (a, c, e, g), in experiment group, upper articular cavity was filled with inflammatory secretions (b, m) and synovial cells apparent hyperplasia (d, f) (arrow head), abundant mononuclear cells (m, n) and lipid droplets (h) (star) were present in the inflammatory synovium. The yellow and red squares in (b) and (d) are magnified in (m) and (n), respectively. EXP: experiment T: temporal bone; D: articular disc; C: condyle; S: synovium.

sc30044, Santa Cruz Biotechnology, Santa Cruz, CA, USA) rabbit anti-OPG (1:100; ab73-400, Abcam, MA, USA) and goat anti-RANKL (1:100; sc7628, Santa Cruz Biotechnology, Santa Cruz, CA, USA) primary antibody overnight at 4°C. The sections were then washed and incubated with immunohistochemical kit (Zhongshan Biotechnology Co., Ltd, China) in compliance with the manufacturer's instructions and visualized by 3,3-diaminobenzidine tetrahydrochloride (DAB). Finally, the sections were counterstained with hematoxylin.

For histometeric measurement, TRAP-positive cells (osteoclasts), OCN-positive cells (osteoblasts), OPG-positive cells and RANKL-positive cells were calculated in five randomly selected magnified fields under an Olympus DP72 microscope by two inspectors and the means of the five measurements was used as the value for this section.

Micro-CT analysis

The samples were scanned by Micro-CT (μCT50, Scanco Medical, Bassersdorf, Switzerland) to examine the TMJ bony change. Scanning was performed at 70 kV and 114 μA with a thickness of 15 μm per slice in medium-resolution mode. The 3D images were reconstructed for quantitative evaluation. The parameters such as bone volume fraction (BV/TV), bone mineral

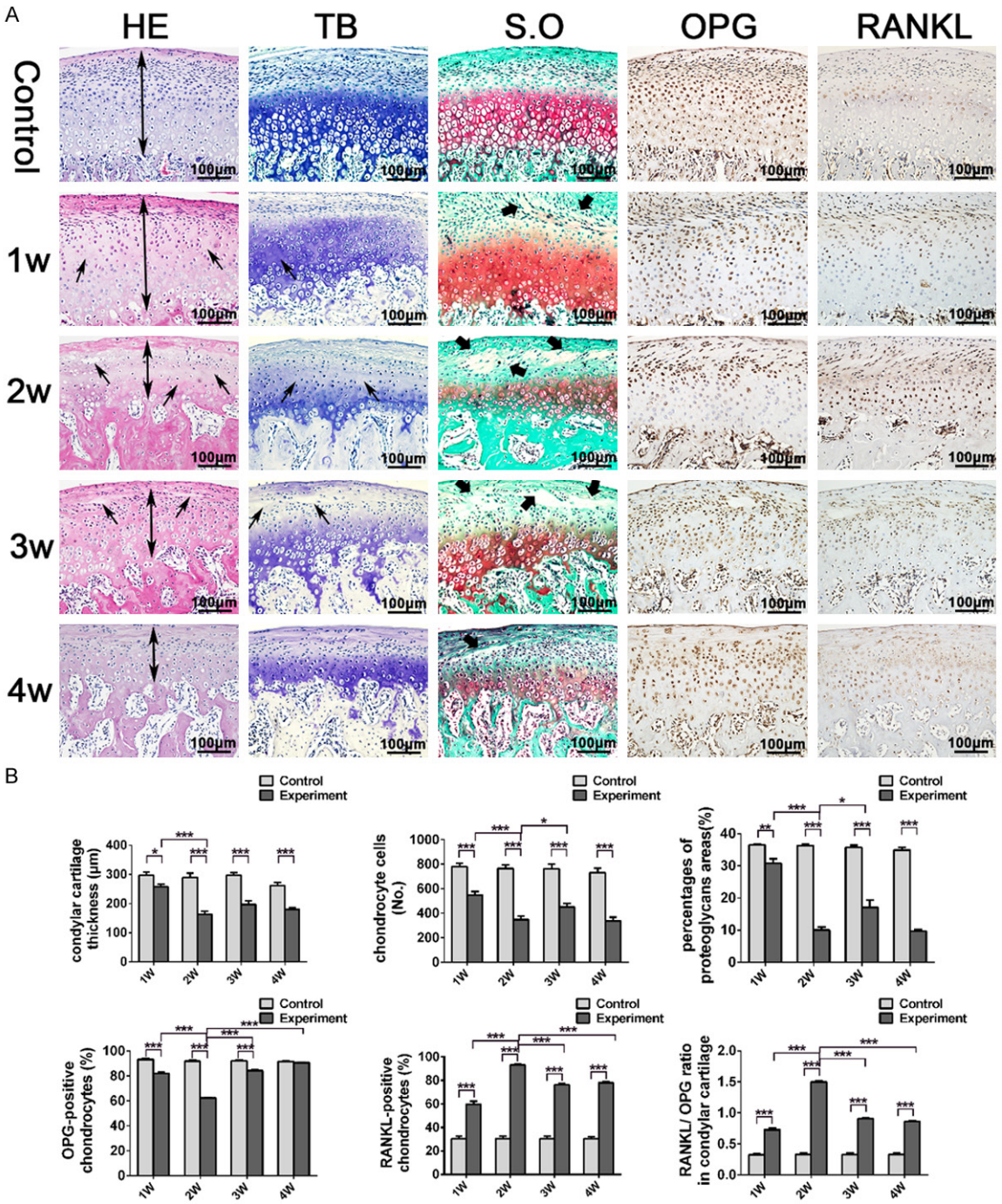

Figure 2. Histological observations and OPG, RANKL expression in TMJ condylar cartilage. A. Representative sections of the condylar cartilage stained with H&E, TB, S.O and OPG, RANKL immunohistochemical staining. B. Comparison between the control and experimental groups in terms of condylar cartilage thickness, number of chondrocytes, extent of proteoglycan degraded areas, percentages of OPG- and RANKL-positive chondrocytes, and RANKL/OPG ratio in condylar cartilage (*p<0.05, **p<0.01, *** p<0.001). Two-way arrow: condylar cartilage thickness. Black arrow: the degraded cartilage areas.

density (BMD), trabecular number (Tb.N), trabecular thickness (Tb.Th), and trabecular separation (Tb.Sp) were measured to analyze trabecular microstructure.

Statistical analysis

All data were presented as the mean ± SEM. Data were analyzed and visualized using GraphPad Prism 6.0. Statistical analysis was performed with two-way analysis of variance (ANOVA). A Student-Newman-Keuls post-test was performed and statistical significance was considered at $p < 0.05$.

Results

Anterior superior puncture technique and rat TMJ inflammation

3D images showed that the needle was situated between the temporal fossa and condyle (**Figure 1Ab**). Severe swelling and chromodacryorrhea were observed 1 day after CFA injection (**Figure 1Bb**) but not detected in the saline injection group (**Figure 1Ba**). The articular upper cavity was filled with inflammatory secretions and mononuclear inflammatory cells (**Figure 1Cb**, **1Cm**). Synovial cells were apparently hyperplasic (**Figure 1Cf**), and a large number of mononuclear cells permeated the synovial membrane (**Figure 1Cd**, **1Cn**). Massive lipid droplets were also present in the inflammatory synovium (**Figure 1Ch**). In the control group, no obvious inflammation was observed (**Figure 1Ca**, **1Cc**, **1Ce**, **1Cg**).

Histological observations

Compared with the control groups, the experimental groups demonstrated gradual decrease in the number of chondrocytes and thickness of the condylar cartilage with time (**Figure 2A**, **2B**) (*$p < 0.05$, ***$p < 0.001$). In the control group, proteoglycans were abundant in the cartilage hypertrophic layer respectively, while the experimental groups exhibited reduced amount of cartilage proteoglycans (**Figure 2A**, **2B**) (*$p < 0.05$, **$p < 0.01$, ***$p < 0.001$). In particular, cartilage thickness, number of chondrocytes and amount of proteoglycans considerably decreased in the 2-week experimental group compared with control group (**Figure 2B**) (***$p < 0.001$).

RANKL and OPG expression in the condylar cartilage

In the control group, OPG-positive chondrocytes were detected in all layers of the condylar cartilage and RANKL-positive chondrocytes were mainly found in the proliferative layer (**Figure 2A**). As the expression level of OPG-positive chondrocytes was higher than that of RANKL, the ratio of RANKL/OPG was reasonably low. In the experimental groups, the numbers of OPG-positive chondrocytes slightly decreased at 1 week, sharply decreased at 2 weeks, and gradually increased thereafter (**Figure 2B**) (***$p < 0.001$). Moreover, OPG-positive chondrocytes were merely observed in the proliferative layer in 2-week experimental group (**Figure 2A**). By contrast, the numbers of RANKL-positive chondrocytes gradually increased and RANKL expression eventually occurred in the entire layer of the cartilage (**Figure 2A**). Accordingly, the RANKL/OPG ratio noticeably increased in the experimental groups particularly at 2 weeks (**Figure 2B**) (***$p < 0.001$).

Subchondral bone remolding in TMJ condyle

No bony changes among the control groups were observed in sagittal slice and 3D image. In the experimental groups, bone lesions were initially observed 1 week after injection, worsened at 2 weeks, and gradually recovered thereafter. At 3 and 4 weeks, the condyle became abnormally shaped and deviated from normal sagittal axis (**Figure 3A**). Within the subchondral bone, larger marrow cavities were observed in the 2-week after injection in the experimental groups (**Figure 3An**). Micro-CT analysis revealed that bone volume fraction (BV/TV), bone mineral density (BMD), trabecular number (Tb.N), and trabecular thickness (Tb.Th) decreased, whereas trabecular separation (Tb.Sp) increased in the experimental groups. The most evident changes were observed in the 2-week group (**Figure 4A**) (*$p < 0.05$, **$p < 0.01$, ***$p < 0.001$).

Mineralized old trabecular bone and unmineralized new bone were stained red and blue, respectively, by Masson trichrome staining. Irregular and disordered trabecular bone structures were observed in the experimental groups (**Figure 4B**). Masson trichrome staining revealed large marrow cavities in the 2-week experimental group (**Figure 3B**). The areas of unmineralized trabecular bone (stained blue) close to the cartilage remarkably increased in the 4-week experimental group (**Figure 4C**) (***$p < 0.001$).

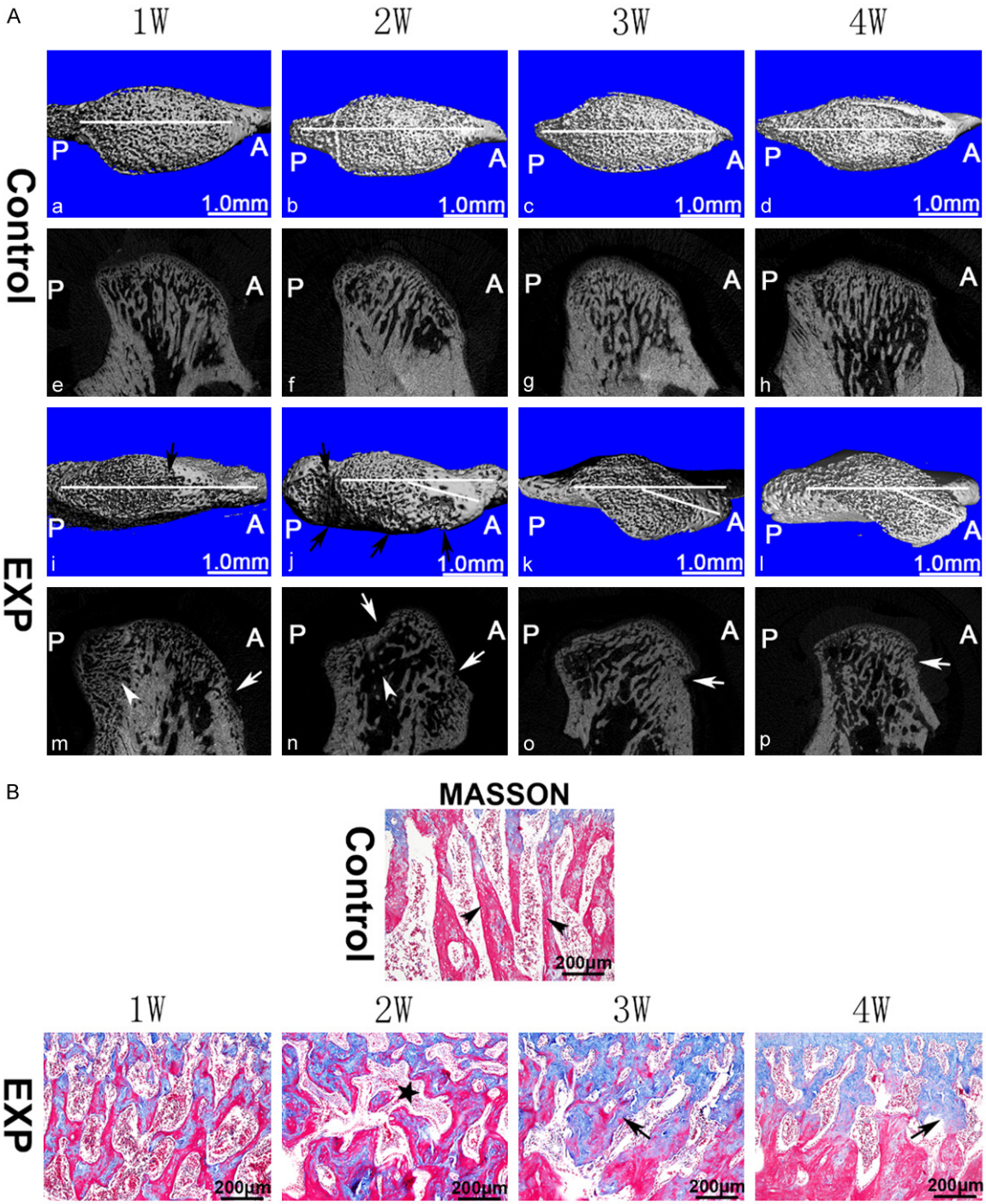

Figure 3. Bony changes in TMJ condyle. (A) Images were arranged from left to right according to the time sequence. In the control group (a-h), the subchondral bone was regularly aligned. Subchondral bone loss (arrows) was observed in the experimental groups (i-p). Generally, regions with lesion were larger (j, n) at 2 weeks than those at other time points. Compared with the control groups (a-d), the 3- and 4-week experimental groups showed obvious atypical condyle shape that deviated from the normal sagittal axis (k, l) based on the 3D reconstruction image. (B) In the control group, normal trabecular bone were long, parallel to each other, and radially perpendicular to the articular surface (arrow head); in the experimental groups, irregular and disordered trabecular bone structure was observed particularly at 3 and 4 weeks (black arrows). The asterisk represents subchondral bone marrow cavity. EXP: experiment, A: anterior, P: posterior. White horizontal line: sagittal axis used for analysis.

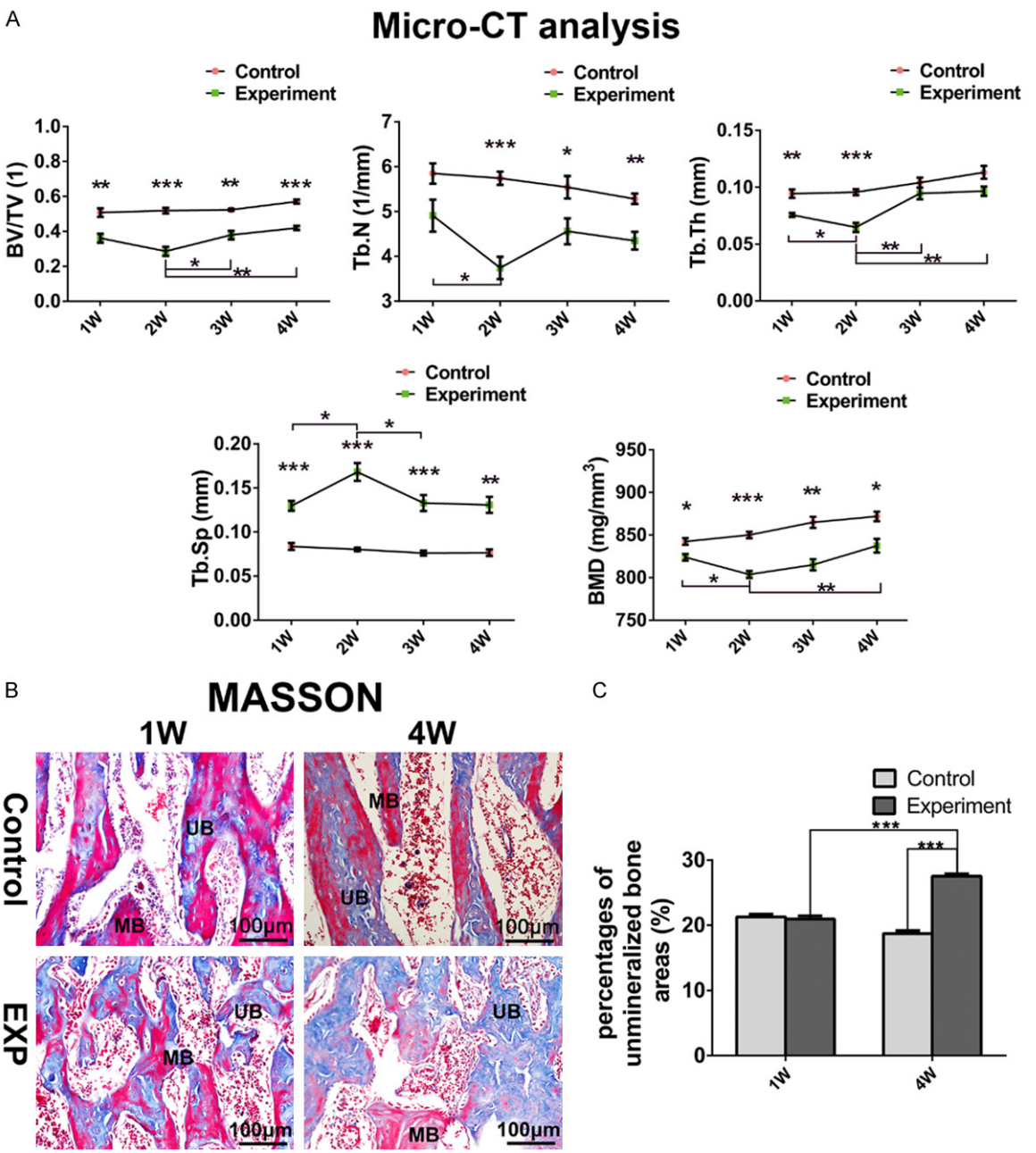

Figure 4. Histomorphometric analysis of condylar subchondral bone. A. micro-CT analysis. B. Representative sections of subchondral bone stained with Masson trichrome. C. Comparison in the percentages of unmineralized bone areas between the experimental and control groups (*p < 0.05, **p < 0.01, *** p < 0.001). EXP: experiment, MB = mineralized bone, UB = unmineralized bone.

Osteoclast and osteoblast activities and RANKL/OPG ratio in Inflamed TMJ subchondral bone

Few cells were positively stained with TRAP in the subchondral bone area in the control groups. In the experimental groups, the number of TRAP-positive cells increased at 1 week, peaked at 2 weeks, and then returned to the normal levels thereafter (**Figure 5A**). OCN-positive cells primarily located on the trabecular bone surface considerably proliferated in the 3- and 4-week experimental groups (**Figure 5A**). The highest RANKL/OPG ratio among the experimental groups was observed at 2 weeks (**Figure 5A**, **5B**) (***p < 0.001).

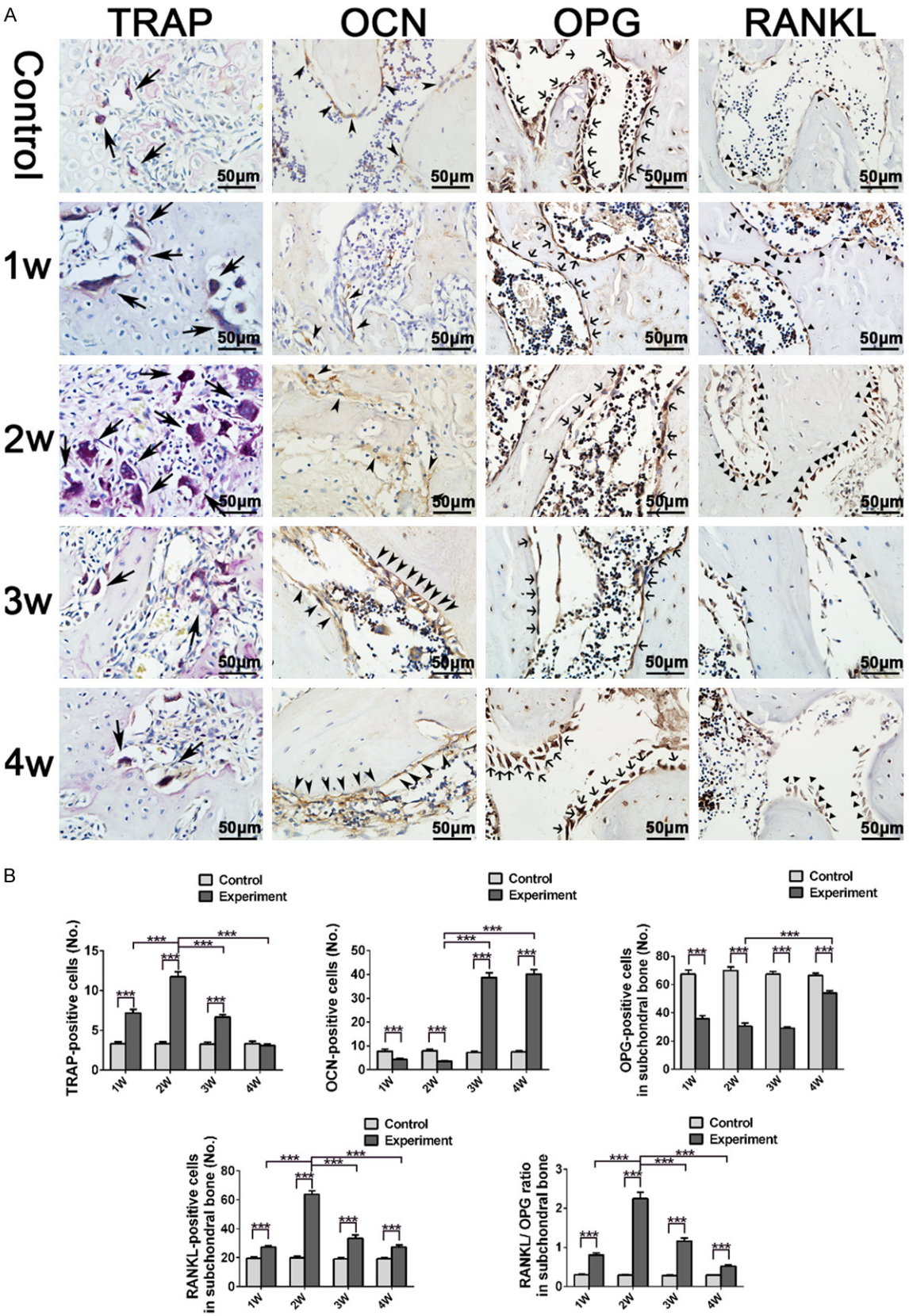

Figure 5. Analysis of osteoclast and osteoblast activities in TMJ condylar subchondral bone. A. Condylar subchondral bone representative sections stained with TRAP, OCN, OPG and RANKL. B. TRAP-positive cells with more than

three nuclei were counted as the number of osteoclasts. The number of OCN-positive, OPG-positive, RANKL-positive cells, and RANKL-positive/OPG-positive ratio was calculated in condylar subchondral bone (***$p < 0.001$).

Discussion

By using the CFA-induced arthritis rat model, we found the time-dependent degeneration manner of TMJ cartilage and subchondral bone, but no progressive cartilage and subchondral bone change related to TMJOA was discovered in this study. The results were correlated with the signs of TMDs. As mentioned before, synovitis in TMJ is one of signs of the TMDs and might lead to TMJOA by cartilage and subchondral bone degradation, but only a few cases of synovitis progressed to OA finally. On the other hand, the time-dependent aberrant changes in condylar cartilage and subchondral bone of inflamed TMJ were found. During inflammation, TMJ degeneration occurred indeed and the degeneration of TMJ reached the peak at 2-week after injection and relived thereafter in this rat model.

In this study, the synovitis was built and swelling and chromodacryorrhea were found in TMJ region. In the 2-week after injection, the RANKL/OPG ratio in the inflamed TMJ condyle reached the peak. The RANKL/OPG system is implicated in cartilage degeneration and subchondral bone remodeling in OA. The increased RANKL/OPG ratio of subchondral bone reveals up-regulated osteoclastic activity and results in bone loss. Moreover, large catabolic molecules from the subchondral bone can permeate into the cartilage region and contribute to cartilage degradation. Similarly, superfluous chondrocyte-originating RANKL diffuse into the subchondral bone region and improve osteoclastic activity, thereby contributing to subchondral bone resorption in OA [19, 22]. Chondrocyte-secreted OPG is an important cytokine that protects the cartilage. OPG deficiency decrease cartilage thickness and enhanced vasculature invasion and chondrocyte apoptosis, which further facilitate molecular crosstalk between the cartilage and subchondral bone [18, 23]. In this study, enhanced RANKL and reduced OPG expression in chondrocytes were accompanied by cartilage degeneration, including reduced number of chondrocytes, thinner condylar cartilage, and degraded proteoglycan areas. Furthermore, increased RANKL and decreased OPG expression levels in the subchondral bone were associated with high osteoclast activity, subchondral bone resorption, and enlarged bone marrow lesions. These findings indicated that in TMJ inflammation, the degeneration in cartilage and subchondral bone happened followed by increased RANKL/OPG ratio.

Subchondral bone remodeling occurs in two phases: predominant bone resorption caused by high osteoclast activity in the early phase and enhanced bone formation with inferior quality in the latter phase [24]. The quality of newly formed bone is highly dependent on subchondral bone turnover. Osteoclast activity, which significantly affects subchondral bone absorption, is regulated by the RANKL/OPG ratio. Furthermore, increased osteoclast activity and RANKL/OPG ratio could improve TMJ subchondral bone turnover in the TMJOA genetic model, whereas improved abnormal bone turnover results in poor quality of the subchondral bone [25-27]. In this study, the maximum osteoclast activity and RANKL/OPG ratio in TMJ subchondral bone was observed in the 2-week experimental group. Accordingly, subchondral bone turnover was enhanced, thereby reducing the quality of subchondral bone. Meanwhile, micro-CT parameters, such as decreased BV/TV, Tb.Th, and Tb.N and increased Tb.Sp, indicated subchondral bone resorption. However, in the 3- and 4-week experimental groups, OCN expression suggesting osteoblast activity sharply increased. At the same time, BV/TV, Tb.Th, and Tb.N subsequently increased but the newly formed bone exhibited lower BMD compared with the age-matched control group. In addition, Masson trichrome staining revealed that the area of unmineralized new bone was larger in the 4-week experimental group than the control group. These results suggested that although the RANKL/OPG ratio decreased after 2-week in experimental group, the effect of inflammation on subchondral bone still sustained.

In this study, the newly formed bone was unmineralized and exhibited poor quality which was consistent with previous studies [24, 28]. The abundant newly formed unmineralized subchondral bone adversely affects tissue properties. Unmineralized bone tissues are character-

ized as decreased modulus of elasticity and more susceptible to deformity under load stress [29, 30]. Actually unmineralized bone tissues provide less resistance and greater compliance than the normal subchondral bone [27, 31]. To adapt to mechanical stress, joint shape and subchondral trabecular bone structure subsequently change according to loads. Abnormal joint shape is regarded as a critical predictor of OA and there is an complicated interactions between them [32]. In this study, micro-CT 3D reconstruction image showed that atypical condylar shape deviated from normal sagittal axis in the 3- and 4-week experimental groups. Meanwhile, Masson trichrome staining further revealed that the normal trabecular bone radial perpendicular to the articular surface was replaced by an irregular and disordered trabecular bone structure.

The experimental groups exhibited decreased proteoglycan amount during inflammation process in a time-dependent manner either in this study. The deceasing of proteoglycan reached the peak at 2-week. Decreased amounts of proteoglycans in the collagen network leads to the low compressive modulus of the condylar cartilage, reduces matrix resistance to compression load, and improves permeability of the cartilage extracellular matrix. Furthermore, cartilage exhibits high deformity under compressive forces [33]. Moreover, previous studies showed that local cartilage damage was associated with bone marrow lesions [18, 34]. In the present study, as the subchondral bone was absorbed by osteoclasts, bone marrow cavity began to merge and gradually increased. Especially, in the 2-week experimental group, prominent condylar cartilage degradation was accompanied with obvious subchondral bone marrow lesions.

Taken together, in this study the time-dependent degeneration manner of cartilage and subchondral bone was found in rat CFA-induced inflamed TMJ model and the relation between inflammation and TMJOA should be clarify in the following studies.

Acknowledgements

This research was supported by National Natural Science Foundation of China (No. 81200804, NO. 81470761, NO. 81401241) and Specialized Research Fund for the Doctoral Program of Higher Education of China (No. 20120141120025). The authors declare no potential conflicts of interest with respect to the authorship and publication of this article.

Disclosure of conflict of interest

None.

Address correspondence to: Drs. Xing Long and Wei Fang, Department of Oral and Maxillofacial Surgery, State Key Laboratory Breeding Base of Basic Science of Stomatology & Key Laboratory of Oral Biomedicine Ministry of Education, School & Hospital of Stomatology, Wuhan University, 237 Luoyu Road, Wuhan, Hubei, China. Tel: +86-027-8768-6216; Fax: +86-027-87873260; E-mail: longxing_china@hotmail.com (XL); fang.wei@whu.edu.cn (WF)

References

[1] Wang XD, Zhang JN, Gan YH and Zhou YH. Current understanding of pathogenesis and treatment of TMJ osteoarthritis. J Dent Res 2015; 94: 666-673.

[2] Wang XD, Kou XX, He DQ, Zeng MM, Meng Z, Bi RY, Liu Y, Zhang JN, Gan YH and Zhou YH. Progression of cartilage degradation, bone resorption and pain in rat temporomandibular joint osteoarthritis induced by injection of iodoacetate. PLoS One 2012; 7: e45036.

[3] Romas E, Gillespie MT and Martin TJ. Involvement of receptor activator of NFkappaB ligand and tumor necrosis factor-alpha in bone destruction in rheumatoid arthritis. Bone 2002; 30: 340-346.

[4] Kapoor M, Martel-Pelletier J, Lajeunesse D, Pelletier JP and Fahmi H. Role of proinflammatory cytokines in the pathophysiology of osteoarthritis. Nat Rev Rheumatol 2011; 7: 33-42.

[5] Siebuhr AS, Bay-Jensen AC, Jordan JM, Kjelgaard-Petersen CF, Christiansen C, Abramson SB, Attur M, Berenbaum F, Kraus V and Karsdal MA. Inflammation (or synovitis)-driven osteoarthritis: an opportunity for personalizing prognosis and treatment? Scand J Rheumatol 2015; 1-12.

[6] Sellam J and Berenbaum F. The role of synovitis in pathophysiology and clinical symptoms of osteoarthritis. Nat Rev Rheumatol 2010; 6: 625-635.

[7] Ke J, Long X, Liu Y, Zhang YF, Li J, Fang W and Meng QG. Role of NF-kappaB in TNF-alpha-induced COX-2 expression in synovial fibroblasts from human TMJ. J Dent Res 2007; 86: 363-367.

[8] Vernal R, Velasquez E, Gamonal J, Garcia-Sanz JA, Silva A and Sanz M. Expression of proin-

flammatory cytokines in osteoarthritis of the temporomandibular joint. Arch Oral Biol 2008; 53: 910-915.

[9] Kou XX, Wu YW, Ding Y, Hao T, Bi RY, Gan YH and Ma X. 17beta-estradiol aggravates temporomandibular joint inflammation through the NF-kappaB pathway in ovariectomized rats. Arthritis Rheum 2011; 63: 1888-1897.

[10] Vos LM, Kuijer R, Huddleston Slater JJ and Stegenga B. Alteration of cartilage degeneration and inflammation markers in temporomandibular joint osteoarthritis occurs proportionally. J Oral Maxillofac Surg 2013; 71: 1659-1664.

[11] Kuroki Y, Honda K, Kijima N, Wada T, Arai Y, Matsumoto N, Iwata K and Shirakawa T. In vivo morphometric analysis of inflammatory condylar changes in rat temporomandibular joint. Oral Dis 2011; 17: 499-507.

[12] Kameoka S, Kuroki Y, Honda K, Kijima N, Matsumoto K, Asano M, Arai Y and Shirakawa T. Diagnostic accuracy of microcomputed tomography for osseous abnormalities in the rat temporomandibular joint condyle. Dentomaxillofac Radiol 2009; 38: 465-469.

[13] Wang XD, Kou XX, Mao JJ, Gan YH and Zhou YH. Sustained inflammation induces degeneration of the temporomandibular joint. J Dent Res 2012; 91: 499-505.

[14] Takayanagi H, Iizuka H, Juji T, Nakagawa T, Yamamoto A, Miyazaki T, Koshihara Y, Oda H, Nakamura K and Tanaka S. Involvement of receptor activator of nuclear factor kappaB ligand/osteoclast differentiation factor in osteoclastogenesis from synoviocytes in rheumatoid arthritis. Arthritis Rheum 2000; 43: 259-269.

[15] Yan JY, Tian FM, Wang WY, Cheng Y, Song HP, Zhang YZ and Zhang L. Parathyroid hormone (1-34) prevents cartilage degradation and preserves subchondral bone micro-architecture in guinea pigs with spontaneous osteoarthritis. Osteoarthritis Cartilage 2014; 22: 1869-1877.

[16] Jiao K, Niu LN, Wang MQ, Dai J, Yu SB, Liu XD and Wang J. Subchondral bone loss following orthodontically induced cartilage degradation in the mandibular condyles of rats. Bone 2011; 48: 362-371.

[17] Liu YD, Liao LF, Zhang HY, Lu L, Jiao K, Zhang M, Zhang J, He JJ, Wu YP, Chen D and Wang MQ. Reducing dietary loading decreases mouse temporomandibular joint degradation induced by anterior crossbite prosthesis. Osteoarthritis Cartilage 2014; 22: 302-312.

[18] Shimizu S, Asou Y, Itoh S, Chung UI, Kawaguchi H, Shinomiya K and Muneta T. Prevention of cartilage destruction with intraarticular osteoclastogenesis inhibitory factor/osteoprotegerin in a murine model of osteoarthritis. Arthritis Rheum 2007; 56: 3358-3365.

[19] Zhu S, Chen K, Lan Y, Zhang N, Jiang R and Hu J. Alendronate protects against articular cartilage erosion by inhibiting subchondral bone loss in ovariectomized rats. Bone 2013; 53: 340-349.

[20] Kameoka S, Matsumoto K, Kai Y, Yonehara Y, Arai Y and Honda K. Establishment of temporomandibular joint puncture technique in rats using in vivo micro-computed tomography (R_mCT(R)). Dentomaxillofac Radiol 2010; 39: 441-445.

[21] Zhang C, Xu Y, Cheng Y, Wu T and Li H. Effect of asymmetric force on the condylar cartilage, subchondral bone and collagens in the temporomandibular joints. Arch Oral Biol 2015; 60: 650-663.

[22] Kadri A, Ea HK, Bazille C, Hannouche D, Liote F and Cohen-Solal ME. Osteoprotegerin inhibits cartilage degradation through an effect on trabecular bone in murine experimental osteoarthritis. Arthritis Rheum 2008; 58: 2379-2386.

[23] Sanchez C, Gabay O, Salvat C, Henrotin YE and Berenbaum F. Mechanical loading highly increases IL-6 production and decreases OPG expression by osteoblasts. Osteoarthritis Cartilage 2009; 17: 473-481.

[24] Zhang J, Jiao K, Zhang M, Zhou T, Liu XD, Yu SB, Lu L, Jing L, Yang T, Zhang Y, Chen D and Wang MQ. Occlusal effects on longitudinal bone alterations of the temporomandibular joint. J Dent Res 2013; 92: 253-259.

[25] Embree M, Ono M, Kilts T, Walker D, Langguth J, Mao J, Bi Y, Barth JL and Young M. Role of subchondral bone during early-stage experimental TMJ osteoarthritis. J Dent Res 2011; 90: 1331-1338.

[26] Embree MC, Kilts TM, Ono M, Inkson CA, Syed-Picard F, Karsdal MA, Oldberg A, Bi Y and Young MF. Biglycan and fibromodulin have essential roles in regulating chondrogenesis and extracellular matrix turnover in temporomandibular joint osteoarthritis. Am J Pathol 2010; 176: 812-826.

[27] Karsdal MA, Leeming DJ, Dam EB, Henriksen K, Alexandersen P, Pastoureau P, Altman RD and Christiansen C. Should subchondral bone turnover be targeted when treating osteoarthritis? Osteoarthritis Cartilage 2008; 16: 638-646.

[28] Bouchgua M, Alexander K, Carmel EN, d'Anjou MA, Beauchamp G, Richard H and Laverty S. Use of routine clinical multimodality imaging in a rabbit model of osteoarthritis--part II: bone mineral density assessment. Osteoarthritis Cartilage 2009; 17: 197-204.

[29] Tanaka E and Koolstra JH. Biomechanics of the temporomandibular joint. J Dent Res 2008; 87: 989-991.

[30] Day JS, Ding M, van der Linden JC, Hvid I, Sumner DR and Weinans H. A decreased subchondral trabecular bone tissue elastic modulus is associated with pre-arthritic cartilage damage. J Orthop Res 2001; 19: 914-918.
[31] Bailey AJ, Mansell JP, Sims TJ and Banse X. Biochemical and mechanical properties of subchondral bone in osteoarthritis. Biorheology 2004; 41: 349-358.
[32] Baker-LePain JC and Lane NE. Relationship between joint shape and the development of osteoarthritis. Curr Opin Rheumatol 2010; 22: 538-543.
[33] Lu XL, Mow VC and Guo XE. Proteoglycans and mechanical behavior of condylar cartilage. J Dent Res 2009; 88: 244-248.
[34] Roemer FW, Guermazi A, Javaid MK, Lynch JA, Niu J, Zhang Y, Felson DT, Lewis CE, Torner J, Nevitt MC and investigators MS. Change in MRI-detected subchondral bone marrow lesions is associated with cartilage loss: the MOST Study. A longitudinal multicentre study of knee osteoarthritis. Ann Rheum Dis 2009; 68: 1461-1465.